A NEURAL NETS URBAN LAND COVER CLASSIFICATION: A CASE STUDY OF BRNO (CZECHIA)

ANDREA KÝNOVÁ, PETR DOBROVOLNÝ

Masaryk University, Faculty of Science, Department of Geography, Czechia

ABSTRACT

Accurate and updated land cover maps provide crucial basic information in a number of important enterprises, with sustainable development and regional planning far from the least of them. Remote sensing is probably the most efficient approach to obtaining a land cover map. However, certain intrinsic limitations limit the accuracy of automatic approaches to image classification. Classifications within highly heterogeneous urban areas are especially challenging. This study makes a presentation of multilayer perceptron (MLP), an artificial neural network (ANN), as an applicable approach to image classification. Optimal MLP architecture parameters were established by means of a training set. The resulting network was used to classify a sub-scene within ASTER imagery. The results were evaluated against a test dataset. The overall accuracy of classification was 94.8%. This is comparable to classification results from a maximum likelihood classifier (MLC) used for the same image. In built-up areas, MLP did not exaggerate built-up areas at the expense of other classes to the same extent as MLC.

Keywords: image classification, multilayer perceptron, urban land cover, ASTER

1. Introduction

Urbanization has an enormous impact on the environment at every scale – local, regional and global (Lu et al. 2008). Anthropogenic land use changes, such as various forms of cultivation, livestock grazing, settlement and construction, reserves and protected lands, and timber extraction, have made cumulative transformations to global land cover (Turner et al. 1994). This in turn influences the environment: climate, biodiversity, soils, water and sediment flow are all in continuous states of change. The urbanization process is very often driven by other interests: nevertheless, efficient urban planning should be based on chronologically and spatially accurate land cover maps (Novack et al. 2011).

Remote sensing provides data and tools which enable the most efficient mapping of urban land cover (Novack et al. 2011). Image classification, the assignation of pixels to selected classes, is one of the basic methods used to generate thematic maps from remote sensing (Vatsavai et al. 2011). Approaches to automatic classification still face certain limitations. Improving the accuracy of land cover classification has attracted a great deal of recent interest in remote sensing studies. Detailed and accurate classification of built-up areas is one of the basic problems, arising out of the enormous spatial and spectral heterogeneity of urban areas, in which built-up structures (buildings, transportation areas), various types of vegetation cover (e.g. parks, gardens, agricultural areas), bare soil zones and bodies of water exist in close proximity (Herold et al. 2002). Definition within built-up areas depends heavily upon the spatial resolution of whatever input images are available. With very high-resolution imagery, every building, road or pavement can be identified and built-up areas are represented as a union of these objects. At a coarser resolution, it is impossible to identify individual objects and individual pixels consist of several types of real-world item (building, road, pavement, garden, forest, soil, etc.). In this case, built-up areas are defined as pixels with prevailing areas of impervious surfaces (including roofs, roads, pavements, car parks, etc.). Spatially and spectrally high and very high-resolution images are not enough to map urban land cover precisely. Improved image classification techniques are of equal importance (Herold et al. 2002).

Recently, several approaches have been suggested that may overcome or suppress some of the features that make it difficult to classify urban land use/land cover correctly using traditional approaches. Thus, for example, subpixel classification reduces the effect of heterogeneity in built-up areas by estimating the composition of a single pixel area (Wu and Murray 2003; Adams and Gillespie 2006; Lu and Weng 2006, 2009; Powell et al. 2007). An object-based approach enables consideration of matters other than spectral characteristics and is particularly useful for classification of very high resolution imagery (Kux and De Pinho 2006; Chen et al. 2007; Cleve et al. 2008; Zhou et al. 2009; Myint et al. 2011; Pu et al. 2011; Dingle Robertson and King 2011). Machine learning methods do not assume any specific theoretical data distribution (Bagan et al. 2008; Yuan et al. 2009; Mountrakis et al. 2011; Sowmya et al. 2011; Rodriguez-Galiano et al. 2012; Jin 2012; Tehrany et al. 2013).

Our study is motivated by the fact that different surfaces (land cover categories) in urban areas significantly influence spatial distribution of air temperature and they

http://dx.doi.org/10.14712/23361980.2015.94
Kýnová, A. – Dobrovolný, P.: A neural nets urban land cover classification: a case study of Brno (Czechia)
AUC Geographica, 50, No. 2, pp. 153–163

contribute directly e.g. to urban heat island formation. Thus land cover maps of urban areas are needed with relatively high precision and in time. This contribution presents artificial neural nets as a non-traditional method of urban land cover classification. In the following section we briefly review recent classification approaches to urban remote sensing. The study area is described in Section 3, together with the classification scheme employed. The available data and a detailed description of the multilayer perceptron algorithm are presented in Section 4. The classification results appear in Section 5, with an evaluation of them and comparison with a statistical classifier in Section 6. Section 7 consists of discussion and our main conclusions appear in Section 8.

2. Review of methods

Remote sensing image analysis acquires the results of a wide range of approaches to land cover mapping that have already been used – with varying degrees of success – in the urban environment. Some of these appear below.

Traditional parametric statistical approaches to supervised classification depend on an assumption of normal data distribution, which may be one of the reasons that they often fail to classify heterogeneous urban areas correctly. Among them, maximum likelihood classifier (MLC) often serves for the evaluation of results arising out of other classification methods, because MLC provides the most accurate results compared to other classifiers (Bishof et al. 1992; Paola and Schowengerdt 1995; Zha et al. 2003; Seto and Liu 2003; Vyorálková 2003; Setiawan et al. 2006).

Methods of spectral enhancement, including the construction of spectral indices (Xu 2007) may be used to extract built-up areas. Spectral indices are usually defined as a simple or normalized ratio of image channels. Normalized difference built-up index (NDBI) has been used for direct extraction of built-up areas (Zha et al. 2003). This is a combination of the short-wavelength infrared (SWIR) and near-infrared (NIR) channels. It is based on the significant increment from NIR to SWIR in the reflectance of built-up areas and barren lands in comparison with only slightly larger or smaller digital number values representing vegetation in the SWIR band than in the NIR band (Zha et al. 2003). NDBI results are often worked up together with other spectral indices, such as the normalized difference vegetation index NDVI (Zha et al. 2003; He et al. 2010), normalized difference water index NDWI, and others (Xu 2007; Uddin et al. 2010). The most serious practical difficulty associated with spectral indices is establishment of the most suitable threshold for extracting built-up areas (He et al. 2010).

Subpixel classification may also be employed when urban land cover is mapped by means of remote sensing. The original specific three-dimensional "vegetation – impervious surface – soil" (V-I-S) model was presented by Ridd (1995), in which classes of urban land cover may be modelled as fractions of vegetation, impervious surface and soil (Wu and Murray 2003). Setiawan et al. (2006) made a comparison between V-I-S and MLC. The overall accuracy achieved by the subpixel approach was 80%, as against 53% for MLC. For estimating impervious surfaces, spectral mixture analysis is the technique most frequently used (Roberts et al. 1998; Wu and Murray 2003; Adams and Gillespie 2006; Lu and Weng 2006, 2009; Powell et al. 2007). This is based on the "un-mixing" of individual land cover fractions, and thus utilizes the same concept as the V-I-S model.

Object-oriented classification is based on segmentation of the original image, dividing the image into groups of neighbouring pixels (objects). These objects are homogenous according to previously-defined criteria. Subsequently, these objects may be classified according to their spectral properties, as well as textural and spatial characteristics. The object-oriented approach allows images of various spatial resolutions to be classified. It is often used in conjunction with very high-resolution sensors (Herold et al. 2002; Kux and De Pinho 2006; Myint et al. 2011; Pu et al. 2011), and for aerial data (Cleve et al. 2008; Zhou et al. 2009). Object-based classification of urban land cover has been tested with high-resolution Landsat data (Dingle Robertson and King 2011) and ASTER data (Chen et al. 2007).

Recently, machine learning algorithms, such as Random Forest (Rodriguez-Galiano et al. 2012; Jin 2012), Support Vector Machine (Mountrakis et al. 2011; Tehrany et al. 2013) and Artificial Neural Networks (ANNs – Bagan et al. 2008; Yuan et al. 2009; Sowmya et al. 2011), have been applied to urban land cover classification (Vatsavai et al. 2011). These approaches can perform at both per-pixel and subpixel levels (Walton 2008) and be used in object-based classification (Smith 2010). One of their advantages for urban land cover classification is independence from theoretical data distribution.

This contribution presents an example of classification employing the multilayer perceptron (MLP) algorithm with application of the back-propagation learning rule. MLP is one of the ANNs based on (presumed) human brain processing; its basic principles appear in section 4.2. As previous studies have shown (Paola and Schowengerdt 1995; Mustapha et al. 2010), the MLP algorithm can achieve higher classification accuracy than the maximum likelihood method. Recently, certain authors (among them Hu and Weng 2009; Sun et al. 2011; Da Silva Brum et al. 2013) have combined or compared the MLP approach with other machine learning algorithms.

3. Study area and classification scheme

Brno is the second largest city in the Czech Republic and the administrative centre of the South Moravian Region [*Jihomaravský kraj*]. In 2002, when the data used in this study were acquired, Brno had a population of over

Fig. 1 The city of Brno in ASTER imagery, acquired on 2 April 2002; band VNIR 1.

370,000. Figure 1 shows the extent of its built-up area and a distribution of main land cover types as they appear in the ASTER imagery that was used for analysis in this paper.

The city is situated in complex terrain at the confluence of two rivers. Natural and anthropogenic surfaces create a rich mosaic, highly influenced by local topography. The historically earlier built-up areas are concentrated in the river valleys. The city has progressively expanded onto its surrounding slopes and also into the lower hills, where the most of housing estates are located (Figure 1). The complexity of terrain has always prevented the creation of a compact city. About 28% of the city administrative area is covered by forests, located mainly at higher altitudes to the north and west of the city. Agricultural fields and large industrial areas occupy the lowland southerly part of the study area, with a number of arterial highways.

Five main land cover types were defined in the study area: built-up areas, agricultural areas, bare soils, forest areas and bodies of water. Built-up areas, the extraction of which is the aim of this classification, include densely built-up areas in the old city centre and housing estates at the edge of the town, suburban built-up areas, and contiguous industrial areas. Other land-cover types were selected in a general way to refine the built-up area extraction. Agricultural areas take the form of fields surrounding the city boundary, especially to the south. Fields differ mainly in volume of vegetation and water content; the category of bare soils is largely represented by quarries. Forest areas include deciduous and coniferous forests located mainly in the northern part of the study area, as well as city parks characterized by a lower density of trees. Bodies of water include larger rivers and several small ponds.

4. Data and methodology

4.1 ASTER Data

The advanced space-borne thermal emission and reflection radiometer (ASTER) imagery used in this study was acquired on the 24th of June 2005. Original VNIR and SWIR images were rectified using a second-order polynomial transformation. All bands of VNIR and SWIR images at 30-m spatial resolution were merged into a single file.

The original image of nine bands (three VNIR and six SWIR) was cropped to the study area. VNIR bands represent the intensity of green, red and near-infrared radiation (wavelength range 0.5–0.9 μm) detected by the VNIR subsystem. The SWIR subsystem acquired six bands at near-infrared wavelengths (1.6–2.43 μm). The next step involved calculation of the divergence statistic that is used as a measure of inter-band correlation (Narendra and Fukunaga 1977) and which may also be used to reduce the number of bands required for a classification. This approach selects bands of the highest discrimination between the categories classified. This is important for the ANN-based method, because reduction of the number of bands determines the size and architecture of the neural net and may significantly reduce its learning time. However, in this study, the net designed for different band subsets according to divergence statistics did not achieve better results compared to the original set of nine bands. All nine VNIR and SWIR bands were therefore employed.

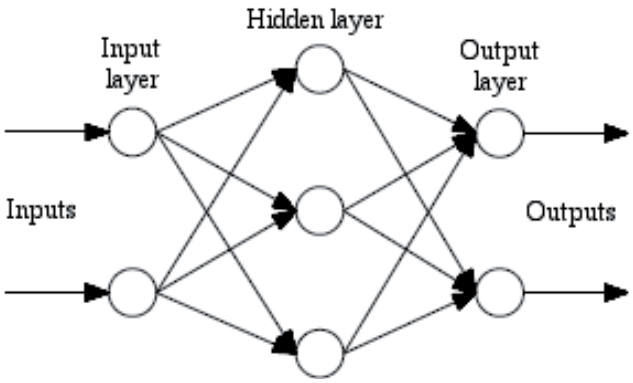

Fig. 2 An example of MLP architecture.

4.2 Multilayer perceptron

The MLP algorithm was applied for land-cover classification. MLP consists of a number of interconnected processing units, arranged in three layers – input layer, one or more hidden layers, and output layer. This arrangement of units is known as the network architecture (Figure 2).

The network architecture was designed in terms of four main parameters: the number of input units, the number of hidden layers, the number of units in each of them and the number of output units. Input units present the bands selected, and possibly other parameters of the image (such as a texture). Each feature may be represented by one or more input units. If more units are used to present a single feature, the range of feature values is divided uniformly; such division can provide enough differences to separate similar values (Bischof et al. 1992).

The numbers of hidden layers and the numbers of their units also affect overall classification accuracy (Foody and Arora 1997). It is recommended to use one or two hidden layers (Šíma and Neruda 1996). An increase in the number of hidden layers enables the network to deal with more complex problems, but is associated with reduction of the ability to generalize and an increase in training time (Foody 1995). According to Lippmann (1987), if two hidden layers are used, the number of units in the second hidden layer should not exceed three times the number of units in the first hidden layer.

The number of output units is usually equal to the number of categories in the classification (Atkinson and Tatnall 1997). Some researchers suggest the use of a greater number of output units to enhance classification accuracy (Benediktsson et al. 1993).

The main principle of ANN is what has become known as the "feed-forward" concept. An input pattern is presented to the network via the input layer and the signals are passed to the neurons of the next layer. The signal is modified along its path through the network by weights associated with neuronal connections. Each receiving neuron sums up weighted signals from all neurons in the preceding layer to which it is connected. The output of a given neuron is computed as a function (usually a non-linear sigmoid function) of the sum of its inputs. When the signal reaches the output layer it becomes network output. In established hard classification the output of one neuron in the output layer (representing one chosen class) is set to one, and the outputs of all other neurons are set to zero.

A network of selected architecture was trained by means of a training set of pixels to set the weights associated with neuronal interconnections. The aim of training is to build a model that can predict outputs from inputs it has never seen before. This property is known as generalization. The back-propagation learning algorithm, described originally by Rumelhart et al. (1986), was used to train the network. A training pattern is presented to the network and the signals are forward-fed via weighted interconnections. The weights are initially set to a random value. The input net_j of a single neuron of the network is computed as a weighted sum of all the inputs it receives and a numerical value, bias b_j (representing a usually-negative threshold value for the unit activation), is added to the sum. Formally, this can be stated as:

$$net_j = \sum_{i=1}^{n} w_{ji} o_i + b_j$$

where n is the number of units in the preceding layer, w_{ji} is the weight associated with the connection between the receiving unit j and the unit i of the preceding layer, while o_i is the output signal of the unit i. The output o_j of a given unit j is computed as a function of the sum according to:

$$o_j = f(net_j) = \frac{1}{1 + e^{-net_j}}$$

The network output is then compared to the desired output and the net partial error E_i is calculated as:

$$E_i = \frac{1}{2} \sum_{j=1}^{k} (o_{ij} - t_{ij})^2$$

where k is the number of categories (number of units in the output layer), o_{ij} is the current output of an output unit j and t_{ij} is the proper output of this unit. The sum of net partial errors for the whole training set provides the total error E of the net. The error is then back-propagated and weights are altered to minimize it. This process is repeated until the computed error drops below a predetermined value or the number of iterations exceeds a predefined maximum.

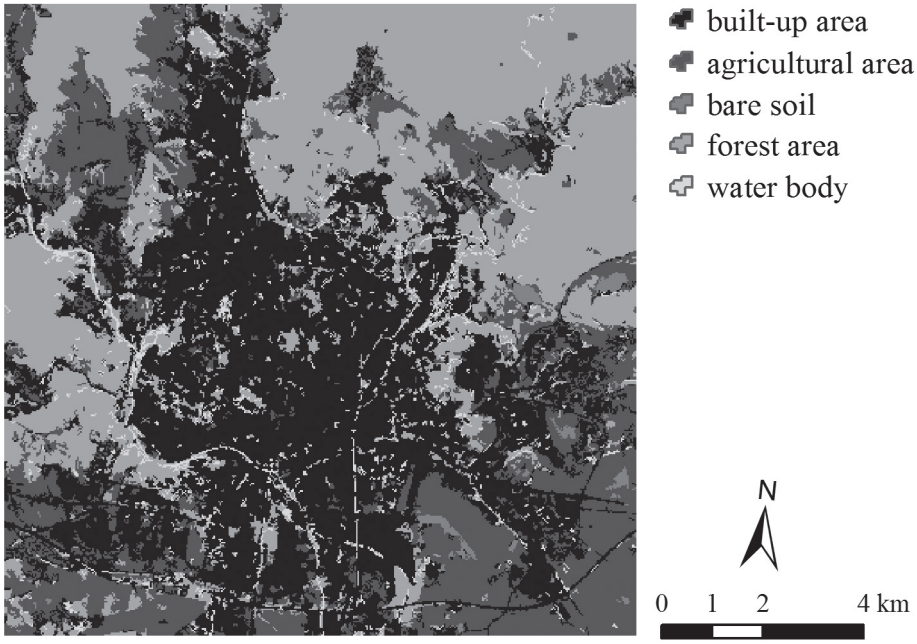

Fig. 3 Land cover of the Brno area as classified from ASTER imagery using MLP.

5. Results

Several ANN architectures, with different numbers of input units, of hidden layers and their units and different numbers of output units, were tested minimize total error and ensure maximal classification accuracy. The best results were obtained using three units per input channel, when the value range is divided into thirds. It follows that the input layer consists of 27 units. Networks tested with only one hidden layer failed to reduce total error to the desired degree. The use of more than two hidden layers mean that networks lose the ability to generalize – the value for total error decreased successfully during the training phase, but the classification accuracy did not achieve a satisfactory value. This trend is known as overfitting. Optimal results were achieved using two hidden layers. The first hidden layer contained 27 units and the second 11 units. The output layer of the optimal network architecture contained the five units that correspond to the individual land cover classes (see Section 4.2). The results of ANN classification appear in Figure 3.

Comparison of classification results (Figure 3) and the original data (Figure 1) indicates that the outer boundaries of built-up areas were identified satisfactorily. Roads were correctly assigned to the built-up area class. Continuous internal parts of the city are disrupted by discrete pixels of agricultural areas, bare soils and bodies of water. Pixels that were incorrectly classified as agricultural areas and bare soils tended to be those of large areas covered by impervious surfaces without vegetation. Pixels incorrectly assigned to bodies of water were often shaded areas.

The classification results were first inspected by simple visual comparison. Figures 4, 5 and 6 compare the built-up areas extracted using MLP with those delimited from very high-resolution aerial photography in three different environments. Figure 4 shows built-up area extraction in the densely built-up city centre. Parks and other larger vegetated areas (site 1 in Figure 4 on the right) are clearly delineated in a continuous street network. In contrast, small or linear parks (site 2) were not all recognised due to the coarser resolution of the image analysed. In Figure 5, a housing estate on the outskirts is presented for

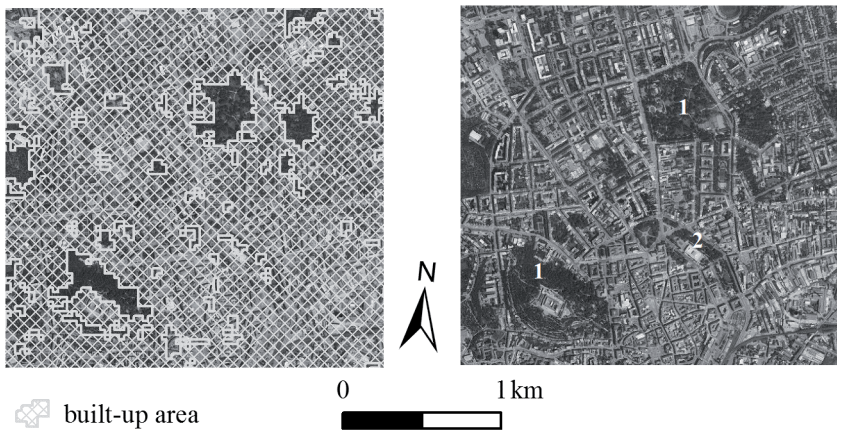

Fig. 4 Built-up areas extracted by classification (a) compared with aerial photography (b: source: WMS geoportal.cuzk.cz) of the city centre; see text for site numbers explanation.

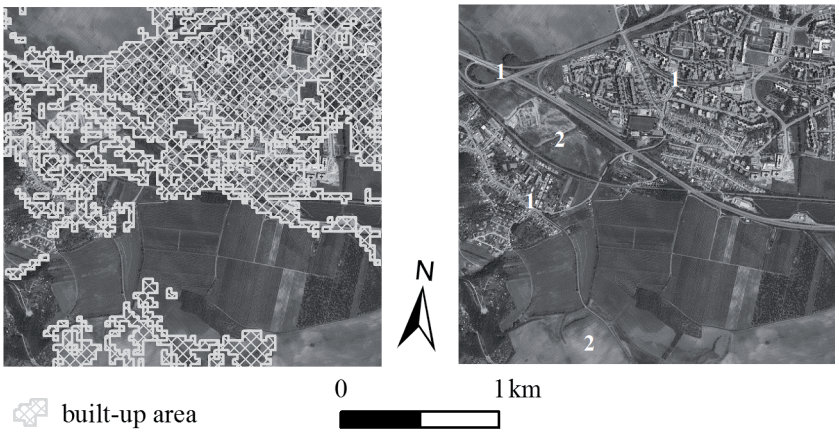

Fig. 5 Built-up areas extracted by classification (a) compared with aerial photography (b: source: WMS geoportal.cuzk.cz) of a housing estate on the outskirts; see text for site numbers explanation.

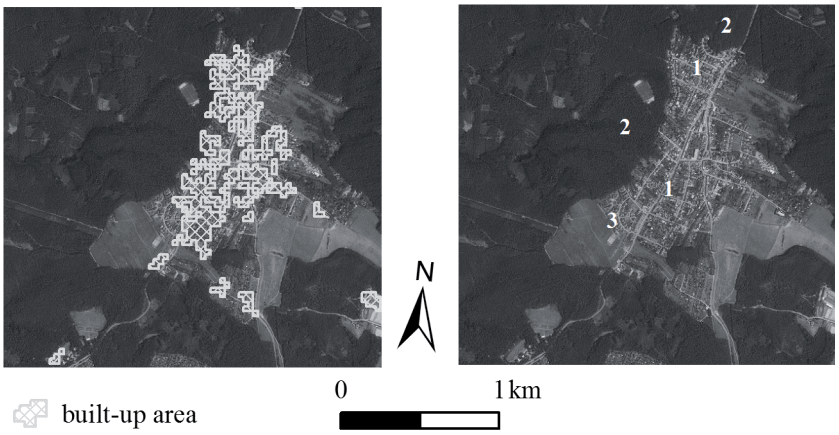

Fig. 6 Built-up areas extracted by classification (a) compared with aerial photography (b: source: WMS geoportal.cuzk.cz) of the city suburbs; see text for site numbers explanation.

comparison. Buildings and roads are correctly assigned to built-up areas (site 1 in Figure 5 on the right). However, certain parts that are in fact fields are inaccurately classified as built-up areas as well (site 2). Finally, Figure 6 shows the extraction of built-up areas in the suburban part of the city. Impervious surfaces representing built-up areas are identified with considerable success (site 1 in Figure 6 on the right). Gardens are correctly assigned to agricultural areas. A sharp boundary between built-up areas and forests is also visible in Figure 6 (site 2). A few buildings in the south-east are not assigned to built-up areas (site 3). These sites were under construction at the time of imagery acquisition and this construction zone was assigned to "bare soils".

Tab. 1 Confusion matrix of a test dataset, comparing class assigned to pixel by the MLP classification and an appropriate class (abbreviations explained in text).

Class		Test dataset					Sum	UA [%]
		1	2	3	4	5		
Classified data	1	**786**	6	4	0	1	797	**98.62**
	2	33	**732**	1	2	0	768	95.31
	3	8	2	**185**	0	0	195	94.87
	4	5	15	0	**1041**	10	1071	97.20
	5	24	0	1	42	**66**	133	49.62
Sum		856	755	191	1085	77	**2964**	–
EO [%]		8.18	3.50	3.14	4.60	14.29	–	–
EC [%]		1.29	4.77	5.24	2.76	87.01	–	–
PA [%]		**91.82**	96.95	96.86	95.94	85.71	–	–

Classes: 1 – built-up area, 2 – agricultural area, 3 – bare soil, 4 – forest area, 5 – body of water.

6. Verification of results

The classification results were verified more formally and objectively in two ways. First, using an independent test dataset and confusion matrix. For an independent test, ground-truth data were divided into two parts. The first one was used for ANN training while the second one was used for validation of results (Section 6.1). Second, the same image was classified in terms of MLC and the results compared to MLP classification results (Section 6.2).

6.1 Evaluation of results

For the MLP classification results, a confusion matrix was computed according to an independent test dataset (Table 1). Five different measures of accuracy were derived – an error of omission (EO), an error of commission (EC), user accuracy (UA), producer accuracy (PA) and overall accuracy: definitions for these appear in, for example, Foody (2002).

An error of omission consists of the percentage of single-class pixels assigned to incorrect classes by classification. In the extraction of built-up areas, about 8% of the pixels were assigned to other classes, mainly to the agricultural area group. The highest error value (nearly 15%) occurred in the class containing bodies of water, as 10 pixels of a total of 77 test pixels in this class were classified as forests. The level of error of commission, specifying the number of pixels incorrectly assigned to a specific class, is very high (nearly 90%) for the water body class, to which 42 pixels of forest area and 24 pixels of built-up area were assigned. Such confusion between bodies of water and forested area arises largely out of the deep shadow thrown in forests. User accuracy defines the ratio of correctly-classified pixels to all pixels as assigned to specific classes. The highest value was derived for built-up areas; nearly 99% of pixels assigned to them truly belong to built-up areas. Except in the class covering bodies of water, user accuracy was around or over 95% for every class. Only one in two pixels assigned to water bodies represented an actual body of water. Producer accuracy describes the numbers of pixels in each class classified correctly. More than 95% of pixels for agricultural and forest areas and bare soils were assigned to the corresponding, correct class. The overall accuracy of the MLP classification was almost 95%.

6.2 Comparison with MLC

For maximum likelihood classification, the original five classes (Section 3) were divided into 11 sub-classes based on differences within categories. The built-up class was divided into three sub-classes. The first consisted of industrial and commercial areas characterized by large, continuous areas of impervious surface, such as concrete, asphalt, etc. The second corresponded to areas with a high density of buildings in the city centre and the third covered suburban areas of houses with gardens. The same set of training pixels as that employed for the MLP classification was used. Training pixels were assigned to sub-classes.

The sub-classes were aggregated into the original five categories and the results evaluated by means of the same independent test dataset as the MLP classification. The overall accuracy was similar (94.5%) to the MLP classification. The error of omission was lower (4.3%) in built-up areas in the MLC classification. However, the error of commission was higher (4.7%). The user accuracy of MLC was 95.3%, in comparison with 98.6% in MLP classification. Altogether, this means that almost 5% of the pixels assigned to built-up areas actually belonged to different classes. In producer accuracy, MLC gave a higher percentage (95.7%) than MLP. A greater difference occurred in error of commission and producer accuracy for bodies of water. In MLC, the error of commission was 5% higher than in MLP and producer accuracy was 4% lower. The producer and user accuracies for most of the classes in MLP (Figure 7) were slightly higher than those in MLC.

A comparison of the overall area assigned to each class by MLC and MLP showed that MLC exaggerated built-up areas at the expense of other classes. MLP classified 36.5% of the image as built-up area, while MLC assigned 43.6% of all pixels to this class.

7. Discussion

The neural network of MLP used in this study to extract built-up areas performed slightly better than statistical MLC. The MLC approach aims to define the subspaces in feature space corresponding to classified categories using parameters of normal distribution computed from a training set. Hence it fails correctly to classify highly heterogeneous built-up areas, which often deviate

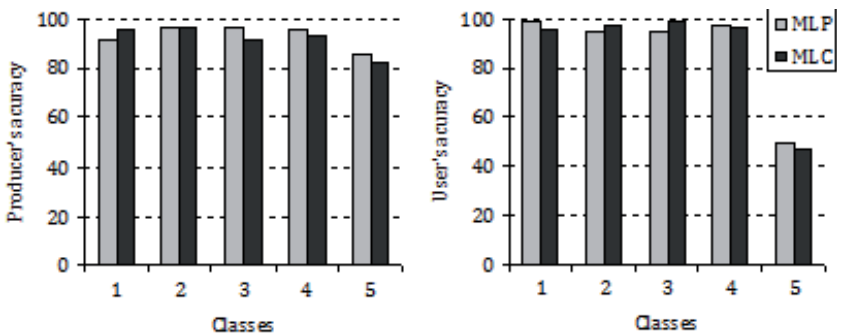

Fig. 7 Comparison of producer and user accuracy of MLP and MLC classification computed for all classes. 1 – built-up area, 2 – agricultural area, 3 – bare soil, 4 – forest area, 5 – body of water.

from "normality". In contrast, MLP does not assume any specific theoretical distribution. Moreover, MLP training attempts to define boundaries between classes in feature space. Boundaries can best be established using atypical representatives of class pixels, independent of value distribution. In this study, the same training set of typical representatives was used for both classifications. This may have partly biased the result of comparison and may be behind the fact that differences in classification accuracy are only slightly significant.

Our analysis related to the design of ANN demonstrated that the accuracy of MLP classification results is influenced to a large extent by ANN architecture. If a network has more than one input neuron for each input channel, it may capture slight differences between the inputs. As presented in Section 5, a topology with three input neurons per channel was used in this study. However, the use of more is far from uncommon, e.g. Benediktsson et al. (1990) used eight neurons and Bischof et al. (1992) used 13 neurons for each input channel. The number of hidden layers also influences network classification performance. A training phase for a smaller network can lead to a deadlock in the local minimum of total error function and the desired error value will not be achieved. Networks with a large number of neurons and hidden layers generally converge rapidly during the training phase, but there is considerable risk of overfitting. An overfitted network is capable of correct classification of a training set but cannot correctly assign pixels it has never seen before. It is therefore necessary to seek the network architecture most appropriate to the particular problem.

In general, MLP classification can be improved by objective selection of the bands required for classification (Kavzoglu and Mathers 2003; Sotoca et al. 2007). Reduction of the number of input bands may serve to emphasize important information in the image. Further, it entails a reduction of units in the neural net and subsequently a reduction in the time required for net training. Transformation of original bands with, for example, principal components, may also enhance important information and suppress noise in the image classified. Band selection based on divergence statistics was used in this contribution, but it did not improve classification accuracy (Section 4.1). ANNs enable the inclusion into classification of data from various sources. In the case of urban land-cover classification, texture information derived from the original image may also help distinguish highly heterogeneous built-up areas from other land cover types (Berberoglu et al. 2007).

Despite its successful classification results, the use of ANNs is still comparatively limited. Empirical rules (e.g. Atkinson and Tatnall 1997; Mather 1999) for determining the number of layers and their neurons are usually overestimated and generate over-large networks prone to overfitting. A large topology can usually be pruned. However, definition of the optimal fitting architecture is still a trial-and-error process (Wilamowski 2009). The time required to train a net may be shortened using more effective computers, through parallel computing, or with faster learning algorithms (Yu and Wilamowski 2009).

8. Conclusion

The need for accurate and up-to-date land cover information has become pressing (Feranec et al. 2007). Spatially and spectrally improved images and sophisticated classification approaches provide tools that eliminate the drawbacks of commonly-used statistical classifiers. Classification results can be further improved by enhancement of specific information in an image with spectral indices and image transformations (Deng et al. 2008; Uddin et al. 2010).

In agreement with several previous studies (e.g. Paola and Schowengerdt 1995; Mustapha et al. 2010), we demonstrated that ANN can address the problem of urban land use/land cover classification as well as, or even better than, statistical approaches and that it does not exaggerate built-up areas as much as a statistical classifier. Thus ANN may be a powerful tool for image classification, but it is still limited by the complex process of finding the best-fitting net architecture (Vatsavai et al. 2011) and a time-consuming and non-deterministic training phase.

The ANN method of land cover classification applied in this case study and our main findings concerning the classification accuracy are related to long-term activities dealing with urban climate of Brno. As different land cover categories contribute differently to air temperature variability and to UHI intensity (Hart and Sailor 2009; Dobrovolný 2013), a compilation of more precise land cover maps is very important. The classification accuracy of the land cover maps directly influences precision of air temperature mapping and subsequently our abilities to mitigate negative consequences of UHI formation. Land cover mapping is important not only in empirically based studies (Dobrovolný and Krahula 2012), but may significantly contribute to urban climate modeling (Hidalgo et al. 2008). Both the land cover map compiled in this case study and the design of the ANN will be further used not only for estimation of UHI intensity but will be also provided to decision maker as a support for sustainable development and for regional planning in Brno area.

Acknowledgements

Andrea Kýnová was kindly supported by Masaryk University project MUNI/A/0952/2013. Authors would like to thank Tony Long (Svinošice) for English style corrections.

REFERENCES

ADAMS, J. B., GILLESPIE, A. R. (2006): Remote sensing of landscapes with spectral images: A physical modeling approach. Cambridge University Press. http://dx.doi.org/10.1017/CBO9780511617195

ATKINSON, P. M., TATNALL, A. R. L. (1997): Introduction Neural networks in remote sensing. International Journal of Remote Sensing 18(4), 699–709. http://dx.doi.org/10.1080/014311697218700

BAGAN, H., WANG, Q., WATANABE, M., KAMEYAMA, S., BAO, Y. (2008): Land-cover classification using ASTER multi-band combinations based on wavelet fusion and SOM Neural Network. Photogrammetric Engineering and Remote Sensing 74(3), 333–342. http://dx.doi.org/10.14358/PERS.74.3.333

BENEDIKTSSON, J. A., SWAIN, P. H., ERSOY, O. K. (1990): Neural network approaches versus statistical methods in classification of multisource remote sensing data. IEEE Transactions on geoscience and remote sensing 28(4), 540–552. http://dx.doi.org/10.1109/TGRS.1990.572944

BENEDIKTSSON, J. A., SWAIN, P. H., ERSOY, O. K. (1993): Conjugate-gradient neural networks in classification of multisource and very-high-dimensional remote sensing data. International Journal of Remote Sensing 14(15), 2883–2903. http://dx.doi.org/10.1080/01431169308904316

BERBEROGLU, S., CURRAN, P. J., LLOYD, C. D., ATKINSON, P. M. (2007): Texture classification of Mediterranean land cover. International Journal of Applied Earth Observation and Geoinformation 9(3), 322–334. http://dx.doi.org/10.1016/j.jag.2006.11.004

BISCHOF, H., SCHNEIDER, W., PINZ, A. J. (1992): Multi-spectral classification of Landsat images using neural network. IEEE Transactions on Geoscience and Remote Sensing 30(3), 482–490. http://dx.doi.org/10.1109/36.142926

CHEN, X. L., ZHAO, H. M., LI, P. X., YIN, Z. Y. (2006): Remote sensing image-based analysis of the relationship between urban heat island and land use/cover changes. Remote sensing of environment 104(2), 133–146. http://dx.doi.org/10.1016/j.rse.2005.11.016

CHEN, Y., SHI, P., FUNG, T., WANG, J., LI, X. (2007): Object-oriented classification for urban land cover mapping with ASTER imagery. International Journal of Remote Sensing 28(20): 4645–4651. http://dx.doi.org/10.1080/01431160500444731

CLEVE, C., KELLY, M., KEARNS, F. R., MORITZ, M. (2008): Classification of the wildland–urban interface: A comparison of pixel- and object-based classifications using high-resolution aerial photography. Computers, Environment and Urban Systems 32(4), 317–326. http://dx.doi.org/10.1016/j.compenvurbsys.2007.10.001

DA SILVA BRUM, V., GARCIA, L. M., KORTING, T. S., DUQUE, C. M. (2013): Intraurban land cover classification using IKONOS II images and data mining techniques: a comparative analysis. In: Urban Remote Sensing Event (JURSE), 2013 Joint. IEEE, 214–217. http://dx.doi.org/10.1109/JURSE.2013.6550703

DENG, J. S., WANG, K., DENG, Y. H., QI, G. J. (2008): PCA-based land-use change detection and analysis using multitemporal and multisensor satellite data. International Journal of Remote Sensing 29(16), 4823–4838. http://dx.doi.org/10.1080/01431160801950162

DINGLE ROBERTSON, L., KING, D. J. (2011): Comparison of pixel- and object-based classification in land cover change mapping. International Journal of Remote Sensing 32(6), 1505–1529. http://dx.doi.org/10.1080/01431160903571791

DOBROVOLNÝ, P. (2013): The surface urban heat island in the city of Brno (Czech Republic) derived from land surface temperatures and selected reasons for its spatial variability. Theoretical and Applied Climatology 112(1–2), 89–98. http://dx.doi.org/10.1007/s00704-012-0717-8

DOBROVOLNÝ, P., KRAHULA, L. (2012): Vliv geometrie zástavby na pole teploty vzduchu a intenzitu tepelného ostrova města na příkladu Brna. Meteorologické zprávy, Praha: Český hydrometeorologický ústav 65(2), 51–57.

EFTHYMIADIS, D. A., JONES, P. D. (2010): Assessment of maximum possible urbanization influences on land temperature data by comparison of land and marine data around coasts. Atmosphere 1(1), 51–61. http://dx.doi.org/10.3390/atmos1010051

FERANEC, J., HAZEU, G., CHRISTENSEN, S., JAFFRAIN, G. (2007): Corine land cover change detection in Europe (case studies of the Netherlands and Slovakia). Land Use Policy 24(1), 234–247. http://dx.doi.org/10.1016/j.landusepol.2006.02.002

FOODY, G. M. (1995): Land cover classification by an artificial neural network with ancillary information. International Journal of Geographical Information Systems 9(5), 527–542. http://dx.doi.org/10.1080/02693799508902054

FOODY, G. M. (2002): Status of land cover classification accuracy assessment. Remote sensing of environment 80(1), 185–201. http://dx.doi.org/10.1016/S0034-4257(01)00295-4

FOODY, G. M., ARORA, M. K. (1997): An evaluation of some factors affecting the accuracy of classification by an artificial neural network. International Journal of Remote Sensing 18(4), 799–810. http://dx.doi.org/10.1080/014311697218764

HART, M. A., SAILOR, D. J. (2009): Quantifying the influence of land-use and surface characteristics on spatial variability in the urban heat island. Theoretical and Applied Climatology 95(3–4), 397–406. http://dx.doi.org/10.1007/s00704-008-0017-5

HE, C., SHI, P., XIE, D., ZHAO, Y. (2010): Improving the normalized difference built-up index to map urban built-up areas using a semiautomatic segmentation approach. Remote Sensing Letters 1(4), 213–221. http://dx.doi.org/10.1080/01431161.2010.481681

HEROLD, M., SCEPAN, J., MÜLLER, A., GÜNTHER, S. (2002): Object-oriented mapping and analysis of urban land use/cover using IKONOS data. In: 22nd Earsel Symposium Geoinformation for European-Wide Integration.

HIDALGO, J., MASSON, V., BAKLANOV, A., PIGEON, G., GIMENO, L. (2008): Advances in urban climate modeling. Trends and Directions in Climate Research, Annals of the New York Academy of Sciences, 1146(1), 354–374. http://dx.doi.org/10.1196/annals.1446.015

HU, X., WENG, Q. (2009): Estimating impervious surfaces from medium spatial resolution imagery using the self-organizing map and multi-layer perceptron neural networks. Remote Sensing of Environment 113(10), 2089–2102. http://dx.doi.org/10.1016/j.rse.2009.05.014

JIANG, J., TIAN, G. (2010): Analysis of the impact of land use/land cover change on land surface temperature with remote sensing. Procedia environmental sciences 2, 571–575. http://dx.doi.org/10.1016/j.proenv.2010.10.062

JIN, J. (2012): A Random Forest Based Method for Urban Land Cover Classification using LiDAR Data and Aerial Imagery, M.A. thesis, Geography Department, University of Waterloo.

KAVZOGLU, T., MATHER, P. M. (2003): The use of backpropagating artificial neural networks in land cover classification. International Journal of Remote Sensing, 24(23), 4907–4938. http://dx.doi.org/10.1080/0143116031000114851

KUX, H. J. H., DE PINHO, C. M. D. (2006): Object-oriented analysis of high-resolution satellite images for intra-urban land cover

classification: Case study in São José Dos Campos, São Paulo State, Brazil. In: Proceedings of 1st International Conference on Obgect-based Image Analysis (OBIA 2006), 4–5.

LIPPMANN, R. (1987): An introduction to computing with neural nets. ASSP Magazine, IEEE 4(2), 4–22. http://dx.doi.org/10.1109/MASSP.1987.1165576

LU, D., SONG, K., ZENG, L., LIU, D., KHAN, S., ZHANG, B., ZONGMING, W., JIN, C. (2008): Estimating impervious surface for the urban area expansion: Examples from Changchun, northeast China. The International Archives of the Photogrammetry, Remote Sensing and Spatial Information Sciences 37, 385–391.

LU, D., WENG, Q. (2006): Use of impervious surface in urban land-use classification. Remote Sensing of Environment 102(1), 146–160. http://dx.doi.org/10.1016/j.rse.2006.02.010

LU, D., WENG, Q. (2009): Extraction of urban impervious surfaces from an IKONOS image. International Journal of Remote Sensing 30(5), 1297–1311. http://dx.doi.org/10.1080/01431160802508985

MATHER, P. M. (1999): Computer Processing of Remotely-Sensed Images – An Introduction. 2nd ed., John Wiley and Sons, Hoboken, N. J.

MOUNTRAKIS, G., IM, J., OGOLE, C. (2011): Support vector machines in remote sensing: A review. ISPRS Journal of Photogrammetry and Remote Sensing 66(3), 247–259. http://dx.doi.org/10.1016/j.isprsjprs.2010.11.001

MUSTAPHA, M. R., LIM, H. S., MAT JAFRI, M. Z. (2010): Comparison of neural network and maximum likelihood approaches in image classification. Journal of Applied Sciences(Faisalabad) 10(22), 2847–2854.

MYINT, S. W., GOBER, P., BRAZEL, A., GROSSMAN-CLARKE, S., WENG, Q. (2011): Per-pixel vs. object-based classification of urban land cover extraction using high spatial resolution imagery. Remote Sensing of Environment 115(5), 1145–1161. http://dx.doi.org/10.1016/j.rse.2010.12.017

NARENDRA, P. M., FUKUNAGA, K. (1977): A branch and bound algorithm for feature subset selection. Computers, IEEE Transactions on 100(9), 917–922.

NOVACK, T., ESCH, T., KUX, H., STILLA, U. (2011): Machine learning comparison between WorldView-2 and QuickBird-2-simulated imagery regarding object-based urban land cover classification. Remote Sensing 3(10), 2263–2282. http://dx.doi.org/10.3390/rs3102263

PAOLA, J. D., SCHOWENGERDT, R. A. (1995): A detailed comparison of back-propagation neural network and maximum-likelihood classifiers for urban and land use classification. IEEE Transactions on Geoscience and Remote Sensing 33(4), 981–996. http://dx.doi.org/10.1109/36.406684

POWELL, R. L., ROBERTS, D. A., DENNISON, P. E., HESS, L. L. (2007): Sub-pixel mapping of urban land cover using multiple endmember spectral mixture analysis: Manaus, Brazil. Remote Sensing of Environment 106(2), 253–267. http://dx.doi.org/10.1016/j.rse.2006.09.005

PU, R., LANDRY, S., YU, Q. (2011): Object-based urban detailed land cover classification with high spatial resolution IKONOS imagery. International Journal of Remote Sensing 32(12), 3285–3308. http://dx.doi.org/10.1080/01431161003745657

RIDD, M. K. (1995): Exploring a VIS (vegetation-impervious surface-soil) model for urban ecosystem analysis through remote sensing: comparative anatomy for cities. International Journal of Remote Sensing 16(12), 2165–2185. http://dx.doi.org/10.1080/01431169508954549

ROBERTS, D. A., Gardner, M., Church, R., Ustin, S., Scheer, G., Green, R. O. (1998): Mapping chaparral in the Santa Monica Mountains using multiple endmember spectral mixture models. Remote Sensing of Environment 65(3), 267–279. http://dx.doi.org/10.1016/S0034-4257(98)00037-6

RODRIGUEZ-GALIANO, V. F., Ghimire, B., Rogan, J., Chica-Olmo, M., Rigol-Sanchez, J. P. (2012): An assessment of the effectiveness of a random forest classifier for land-cover classification. ISPRS Journal of Photogrammetry and Remote Sensing 67, 93–104. http://dx.doi.org/10.1016/j.isprsjprs.2011.11.002

RUMELHART, D. E., HINTONT, G. E., WILLIAMS, R. J. (1986): Learning representations by back-propagating errors. Nature 323, 533–536. http://dx.doi.org/10.1038/323533a0

SETIAWAN, H., MATHIEU, R., THOMPSON-FAWCETT, M. (2006): Assessing the applicability of the V–I–S model to map urban land use in the developing world: Case study of Yogyakarta, Indonesia. Computers, Environment and Urban Systems 30, 503–522. http://dx.doi.org/10.1016/j.compenvurbsys.2005.04.003

SETO, K. C., LIU, W (2003): Comparing ARTMAP neural network with the maximum-likelihood classifier for detecting urban change. Photogrammetric Engineering and Remote Sensing 69 (9), 981–990. http://dx.doi.org/10.14358/PERS.69.9.981

SMITH, A. (2010): Image segmentation scale parameter optimization and land cover classification using the Random Forest algorithm. Journal of Spatial Science 55(1), 69–79. http://dx.doi.org/10.1080/14498596.2010.487851

SOWMYA, B., Thirumaran, A., Aravindh, R., Prasad, A. A. (2011): Land cover classification using Adaptive Resonance Theory-2. In: Electronics, Communication and Computing Technologies (ICECCT), 2011 International Conference on. IEEE, 78-82.

SUN, Z., GUO, H., LI, X., LU, L., DU, X. (2011): Estimating urban impervious surfaces from Landsat-5 TM imagery using multilayer perceptron neural network and support vector machine. Journal of Applied Remote Sensing 5(1). http://dx.doi.org/10.1117/1.3539767

ŠÍMA, J., NERUDA, R. (1996): Teoretické otázky neuronových sítí. 1st ed., MATFYZPRESS, Praha.

TEHRANY, M. S., PRADHAN, B., JEBU, M. N. (2013): A comparative assessment between object and pixel-based classification approaches for land use/land cover mapping using SPOT 5 imagery. Geocarto International, ahead-of-print: 1–19.

TURNER, B. L., MEYER, W. B., SKOLE, D. L. (1994): Global land-use/land-cover change: towards an integrated study. AMBIO-STOCKHOLM 23, 91–91.

UDDIN, S., AL GHADBAN, A. N., AL DOUSARI, A., AL MURAD, M., AL SHAMROUKH, D. (2010): A remote sensing classification for land-cover changes and micro-climate in Kuwait. International Journal of Sustainable Development and Planning 5, 367–377. http://dx.doi.org/10.2495/SDP-V5-N4-367-377

SOTOCA, J. M., PLA, F., SÁNCHEZ, J. S. (2007): Band selection in multispectral images by minimization of dependent information. Systems, Man, and Cybernetics, Part C: Applications and Reviews, IEEE Transactions on, 37(2), 258–267.

VATSAVAI, R. R., BRIGHT, E., VARUN, C., BUDHENDRA, B., CHERIYADAT, A., GRASSER, J. (2011): Machine learning approaches for high-resolution urban land cover classification: a comparative study. In: Proceedings of the 2nd International Conference on Computing for Geospatial Research and Applications. ACM.

VYORÁLKOVÁ, I. (2003): Zpracování satelitních snímků neuronovými sítěmi. Automatizace 46(11), 742–745.

WALTON, J. T. (2008): Subpixel urban land cover estimation: comparing cubist, random forests, and support vector regression. Photogrammetric Engineering and Remote Sensing 74(10), 1213–1222. http://dx.doi.org/10.14358/PERS.74.10.1213

WILAMOWSKI, B. M. (2009): Neural network architectures and learning algorithms. Industrial Electronics Magazine, IEEE 3(4), 56–63. http://dx.doi.org/10.1109/MIE.2009.934790

WU, C., MURRAY, A. T. (2003): Estimating impervious surface distribution by spectral mixture analysis. Remote sensing of Environment 84(4), 493–505. http://dx.doi.org/10.1016/S0034-4257(02)00136-0

XU, H. (2007): Extraction of urban built-up land features from Landsat imagery using a thematic-oriented index combination technique. Photogrammetric Engineering and Remote Sensing 73(12), 1381–1391. http://dx.doi.org/10.14358/PERS.73.12.1381

YU, H., WILAMOWSKI, B. M. (2009): Efficient and reliable training of neural networks. In: Human System Interactions, 2009. HSI'09. 2nd Conference on. IEEE, 109–115.

YUAN, H., VAN DER WIELE, C. F., KHORRAM, S. (2009): An automated artificial neural network system for land use/land cover classification from Landsat TM imagery. Remote Sensing 1(3), 243–265. http://dx.doi.org/10.3390/rs1030243

ZHA, Y., GAO, J., NI, S. (2003): Use of normalized difference built-up index in automatically mapping urban areas from TM imagery. International Journal of Remote Sensing 24(3), 583–594. http://dx.doi.org/10.1080/01431160304987

ZHOU, W., HUANG, G., TROY, A., CADENASSO, M. L. (2009): Object-based land cover classification of shaded areas in high spatial resolution imagery of urban areas: A comparison study. Remote Sensing of Environment 113(8), 1769–1777. http://dx.doi.org/10.1016/j.rse.2009.04.007

Andrea Kýnová
Masaryk University
Department of Geography
Kotlářská 2, 611 37 Brno
Czechia
E-mail: 175953@mail.muni.cz

Petr Dobrovolný
Masaryk University
Department of Geography
Kotlářská 2, 611 37 Brno
Czechia
E-mail: dobro@sci.muni.cz

RESUMÉ

Role neuronových sítí při klasifikaci druhů povrchu v zastavěných oblastech: vícevrstvá neuronová síť

Aktuální a přesné mapy druhů povrchů poskytují zásadní informace pro řadu odvětví, mezi jinými pro územní plánování a trvale udržitelný rozvoj. Dálkový průzkum Země nabízí zřejmě nejefektivnější přístup pro tvorbu těchto map. Přesnost metod automatické klasifikace obrazu je nicméně stále limitována, zvláště ve vysoce heterogenních zastavěných oblastech. Tato studie prezentuje vícevrstvou neuronovou síť (multilayer perceptron) jako příklad jednoho z možných přístupů ke klasifikaci obrazu. Optimálního nastavení parametrů architektury použité neuronové sítě bylo dosaženo pomocí trénovací množiny vzorů. Výsledná síť se dvěma skrytými vrstvami byla použita pro klasifikaci satelitního snímku pořízeného senzorem ASTER. Výsledek klasifikace byl následně zhodnocen pomocí testovací množiny dat. Celková přesnost klasifikace vůči testovacím datům dosahovala 94,8 %, což je srovnatelné s klasifikací získanou využitím klasifikátoru maximální pravděpodobnosti (maximum likelihood) pro totožný snímek. Výraznějšího rozdílu v klasifikaci si lze povšimnout především ve výsledné rozloze zastavěných ploch, kdy klasifikátor maximální pravděpodobnosti značně nadhodnotil zastoupení zastavěných ploch v obraze (43,6 %) oproti ostatním klasifikovaným třídám. Klasifikací vícevrstvou neuronovou sítí byla zastavěná plocha vymezena na 36,5 % klasifikovaného území.